7-27-2012

Nanoscale contacts between semiconducting nanowires and metallic graphenes

Seongmin Kim
Purdue University, kim482@purdue.edu

David B. Janes
Purdue University, janes@ecn.purdue.edu

Sung-Yool Choi
KAIST, sungyool.choi@kaist.ac.kr

Sanghyun Ju
Kyonggi University, shju@kyonggi.ac.kr

Follow this and additional works at: http://docs.lib.purdue.edu/nanopub

Part of the Electrical and Electronics Commons, Electronic Devices and Semiconductor Manufacturing Commons, Nanoscience and Nanotechnology Commons, and the Nanotechnology Fabrication Commons

Nanoscale contacts between semiconducting nanowires and metallic graphenes

Seongmin Kim, David B. Janes, Sung-Yool Choi, and Sanghyun Ju

Related Articles

Inhomogeneous ohmic contacts: Barrier height and contact area determination
Appl. Phys. Lett. 101, 051604 (2012)

Ultra-low resistance ohmic contacts to GaN with high Si doping concentrations grown by molecular beam epitaxy
Appl. Phys. Lett. 101, 032109 (2012)

Carrier transport mechanism at metal/amorphous gallium indium zinc oxides interfaces
Appl. Phys. Lett. 101, 033506 (2012)

Effect of metals and annealing on specific contact resistivity of GeTe/metal contacts
Appl. Phys. Lett. 101, 012107 (2012)

Methodology of evaluating the influence of the resistance of contact regions in the measurements of sheet resistance on stripes of ultrathin high-resistance materials
Rev. Sci. Instrum. 83, 074701 (2012)

Additional information on Appl. Phys. Lett.

Journal Homepage: http://apl.aip.org/

Journal Information: http://apl.aip.org/about/about_the_journal

Top downloads: http://apl.aip.org/features/most_downloaded

Information for Authors: http://apl.aip.org/authors

Nanoscale contacts between semiconducting nanowires and metallic graphenes

Seongmin Kim,[1] David B. Janes,[1] Sung-Yool Choi,[2] and Sanghyun Ju[3,a]

[1]*School of Electrical and Computer Engineering and Birck Nanotechnology Center, Purdue University, West Lafayette, Indiana 47907, USA*
[2]*Department of Electrical Engineering, KAIST, Daejeon 305-701, South Korea*
[3]*Department of Physics, Kyonggi University, Suwon, Gyeonggi-Do 443-760, South Korea*

Here we report on the metal–semiconductor junction characteristics of a semiconducting ZnO nanowire grown directly on a metallic graphene film. The extracted specific contact resistivity of the graphene–ZnO nanowire contact (1.5×10^{-5} $\Omega \cdot cm^2$) is comparable to that reported for Al–ZnO contacts. Based on the assumption that thermionic-field emission is the dominant mechanism, we obtained a zero-bias effective barrier height of 0.413 eV for the graphene–ZnO nanowire Schottky contact. We thus demonstrate that as a result of the enhanced tunneling at the contact, the graphene–nanowire contact exhibits near-ohmic current–voltage characteristics with a low contact resistance. © 2012 American Institute of Physics. [http://dx.doi.org/10.1063/1.4745210]

Graphene, a novel material for electronic device applications, has a high electrical conductivity, thermal stability, and optical transparency that make it ideal as a next-generation electrode material.[1,2] The number of investigations employing graphene films as electrodes for a variety of devices has recently increased,[3,4] and while nanowires (NWs) grown directly on graphene without a catalyst have been reported,[5] detailed studies of the contact properties between graphene and NWs are still required. Generally, metals such as Al and Ti, which exhibit work function values (4.28 eV and 4.33 eV, respectively) similar to the ZnO (one representative NW material) electron affinity (4.2 eV), have often been chosen as the electrodes for ohmic contacts to *n*-type ZnO materials. Al and Ti are also well suited since they are chemically reactive to ZnO, creating donor-like oxygen vacancies (V_O) at the metal–ZnO NW interface; this increases the doping concentration at the sub-surface and hence reduces the barrier width.[6,7] However, Al (or Ti) to ZnO contacts show poor thermal stability due to the chemically reactive interface and are often limited to devices operating under low-power and low-temperature conditions.

In this research, a graphene thin film has been employed as a catalytic material for NW growth as well as for electrical wiring and as a low-resistance electrode. ZnO NWs are grown directly on the graphene thin film in order to analyze the contact characteristics of the graphene–ZnO NW interface. The current–voltage (*I–V*) characteristics of the graphene–NW–Al devices have been measured and compared to those of Al–NW–Al devices. A consideration of these two device types allows an estimation of the NW resistivity and the specific contact resistivity of the graphene–NW contact.

Figure 1(a) shows a schematic of the two-terminal device containing a ZnO NW between the multilayer graphene and Al electrodes. The graphene thin film used in this study was fabricated with a Ni catalyst and transferred onto the substrate as in our previous studies.[5] Figure 1(b) shows a high-resolution transmission electron microscopy (HR–TEM) cross-sectional image of the fabricated multi-layer graphene film (MGF) that consisted of approximately 20 graphene layers, with a total thickness of 6–6.5 nm and a sheet resistance and mobility of approximately 200 Ω/sq and 1200 cm²/V·s, respectively. The MGF Raman spectrum (Figure 1(b) inset) measured by Raman microscopy showed that the graphene quality was remarkable; the 2D band has a sharp peak (at 2700 cm^{-1}), the D band has a low peak (at 1350 cm^{-1}), and the 2D/G band ratio is greater than 0.5 (the G band is at 1580 cm^{-1}).

The MGF was then dry etched (O_2) into the 55 µm × 100 µm sized islands required for device fabrication. First, a SiO_2 layer (thickness: 70 nm) was sputter-deposited and patterned by photolithography to protect the areas where the MGF is required. The SiO_2 layer was used as a mask for the O_2 dry etching, and the areas of the MGF that were not covered by the SiO_2 layer were removed after
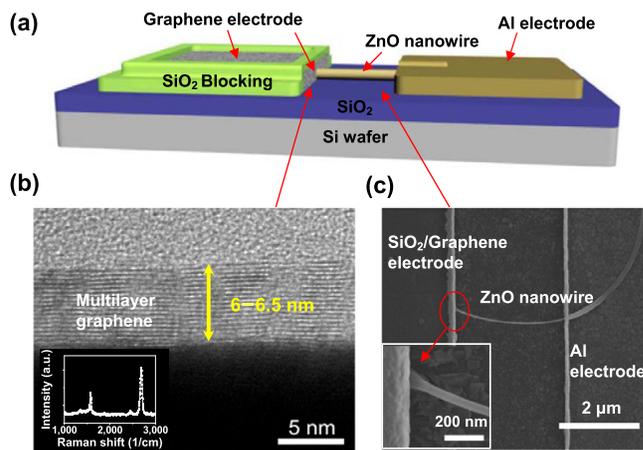

FIG. 1. (a) Schematic diagram of the two-terminal device containing a ZnO NW between the multilayer graphene and Al electrodes. (b) Cross-sectional HR–TEM image of the MGF. The inset shows the MGF Raman spectrum. (c) FE–SEM image of the device. The inset shows an expanded view of the contact region.

a)Author to whom correspondence should be addressed. Electronic mail: shju@kgu.ac.kr.

etching. Consequently, in the final structure, only the edges of the graphene film are exposed.

The NWs were grown horizontally on the substrate, nucleating on the exposed MGF sidewalls. The ZnO source material and patterned graphene substrate were located in separate zones, and the temperatures of the two areas were increased to 1070 °C and 750 °C, respectively. As shown in the inset of Figure 1(c), the ZnO NWs form a metal–semiconductor (M–S) contact with the sidewall of the MGF. It was expected that the NW source material would diffuse on the graphene film surface to form a layer, incorporating high-surface-energy sites on which NWs could grow.[4,5] This occurred and the ZnO NWs were grown from the exposed MGF sidewall.

A 100-nm-thick Al electrode was then deposited and patterned at the other end of the ZnO NW. In this manner, the ZnO NW had a two-terminal structure with one contact (graphene) formed during NW growth and the other contact consisting of post-deposited Al metal (Figure 1(c)). The measured NW diameter (d_{nw}) and length of the channel (L_{ch}) were 50 nm and 3 μm, respectively. In order to compare the properties of the MGF–ZnO NW contacts to the commonly used Al–ZnO NW contacts, we also fabricated a two-terminal device ($L_{ch} \sim 3\,\mu$m) with the same metal (Al) for both source and drain electrodes.

Figures 2(a) and 2(b) show the measured room-temperature I–V characteristics shown on a linear and log scale, respectively, of the two representative two-terminal devices: (i) a ZnO NW connecting the MGF and Al electrodes (MGF–ZnO NW–Al), and (ii) a ZnO NW connecting two Al electrodes (Al–ZnO NW–Al). The Al–ZnO NW–Al device shows a nearly linear I–V relationship in both the for-

ward and negative bias regions. The I–V curve of the MGF–ZnO NW–Al device displays some non-linearity but no severe rectifying behavior in the reverse bias region and exhibits a non-zero slope at $V = 0$.

The fabricated devices, utilizing two different materials as the S–D electrodes, can be modeled three different ways: (1) a NW resistor connected by two ohmic contacts; (2) a NW resistor connected by one Schottky diode and one ohmic contact; or (3) two asymmetric Schottky diodes inversely connected back-to-back and bridging the NW channel. The linear I–V curve of the Al–ZnO NW–Al device implies that both Al–ZnO NW contacts can be modeled as ohmic contacts. When both contacts are ohmic, a resistance (R) of ~175 kΩ can be extracted from the slope of the measured I–V curve following Ohm's law ($V = IR$). Assuming that the ohmic contact resistance is negligible compared to the channel resistance, the doping density of the ZnO NW (N_D) can be estimated as ~1.0×10^{19} cm^{-3} from

$$N_D = \frac{1}{q\mu\rho_s} = \frac{1}{q\mu R}\frac{L_{ch}}{\pi r_{rw}^2}, \qquad (1)$$

where q is the electronic charge, r_{nw} is the NW radius, and μ (~41 cm^2/V·s) is the reported mobility of the ZnO NWs grown from the MGF.[8] Here, the ZnO NW resistivity (ρ_s) is calculated to be ~1.14×10^{-2} Ω·cm. Incorporating a non-zero contact resistance would decrease (increase) the extracted ρ_s (N_D) value. Note that the ZnO NW is not intentionally doped during the growth; however, it is expected to show n-type behavior with high doping concentrations due to the existence of donor-like oxygen vacancies on the ZnO NW surface.[9]

Since the Al–ZnO NW contacts provide a higher conductance and linear I–V curves, the I–V characteristics of the MGF–ZnO NW–Al device in both the forward and reverse bias regions are expected to be dominated by the electrical transport mechanism at the MGF–ZnO NW contact. The upward bending feature of I–V curve in both bias regions suggests that the MGF–ZnO NW contact is not modeled well by an ohmic contact. The MGF–ZnO NW–Al device shows a resistance of approximately 623 kΩ over a voltage range of 0.2–0.4 V. Previous studies have reported that Ti–ZnO NW Schottky diodes exhibit room-temperature resistances in the range of 0.1 to 10 MΩ.[10] The high room-temperature resistance and non-linear I–V curve suggest that the MGF–ZnO NW contact is behaving as a Schottky diode contact with a high contact resistance. Hence, the MGF–ZnO NW–Al device can be modeled as a series connection of a Schottky contact (MGF–ZnO NW) with a large resistance, a NW resistor (ZnO) with the same resistance as that in the Al–ZnO NW–Al device, and an ohmic contact with negligible resistance (ZnO NW–Al). A schematic circuit model of the MGF–ZnO NW–Al device is depicted in Figure 3(b).

Before we analyze the physics in detail, we consider the unique nanostructure of the MGF–ZnO NW contacts. As shown in Figure 3(c), the Schottky contact area (A_C) of the MGF–ZnO NW Schottky contact can be modeled as a disk with the same diameter as the NW (50 nm). A MGF–ZnO NW contact resistivity (ρ_c) of 1.5×10^{-5} Ω·cm^2 can be extracted from
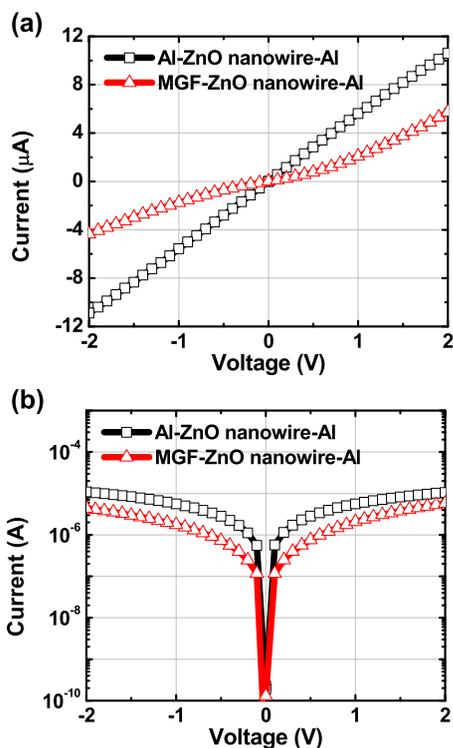

FIG. 2. The two-terminal I–V characteristics of the representative Al–ZnO NW–Al (square) and MGF–ZnO NW–Al (triangle) device on a (a) linear and (b) log scale.
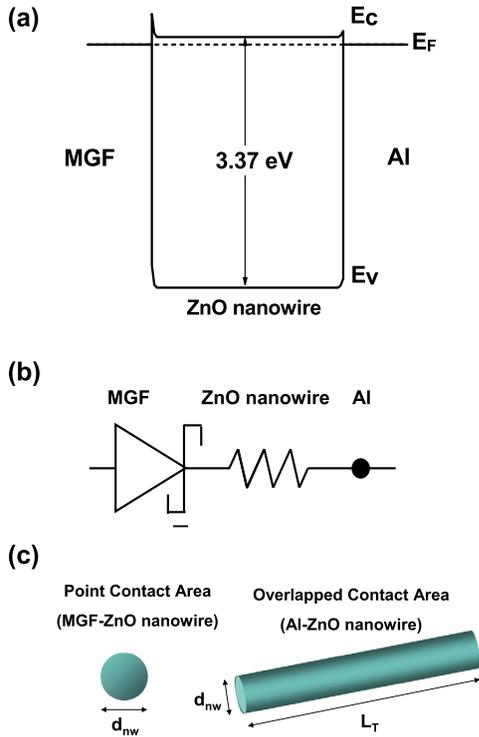
FIG. 3. (a) Schematic band diagram and (b) circuit model of the MGF–ZnO NW–Al device. (c) Illustration of the MGF–ZnO NW and Al–ZnO NW contact areas.

$$R_C = \frac{\rho_C}{A_C} \quad (2)$$

for a measured contact resistance (R_c) of 760 kΩ.

Although the resistance of the Al–ZnO NW contact cannot be extracted directly, it can be estimated from the geometry and the typical value of ρ_c. For the Al–ZnO NW contacts, since the NWs partially overlap the Al electrode, A_C is assumed to be the surface area over which the electrode wraps the cylindrical ZnO NW. The transfer length (L_T) at the contact is expressed as[11]

$$L_T = \sqrt{\frac{r_{nw}\rho_C}{2\rho_S}}. \quad (3)$$

For the Al–ZnO ρ_c values, ranging from $1.2 \times 10^{-5}\,\Omega \cdot cm^2$ to $2.5 \times 10^{-5}\,\Omega \cdot cm^2$, reported in the literature,[6,7] L_T is calculated to be 0.36–0.52 μm. Note that the corresponding R_c value calculated from Eq. (2) is in the range of 7.8–16.3 kΩ, which is self-consistent with the assumption that the contact resistance of the Al–ZnO NW contact is negligible compared to the NW resistance. The estimated L_T values indicate that the effective area of the Al–ZnO NW contact is expected to be 7 to 10 times larger than that of the MGF–ZnO NW contact. According to Eq. (2), the smaller junction area of the MGF–ZnO NW contact is expected to result in a higher contact resistance, and consequently, a lower current compared with that of the Al–ZnO NW contact even if the specific contact resistivity is a similar value. Note that this trend is in good agreement with the I–V curves near zero bias shown in Figure 2(a). The extracted values of ρ_c of the MGF–ZnO NW contact are comparable to or lower than most of the reported *n*-type Schottky barriers using ZnO thin films and

various metals, which is consistent with the low resistances observed in the I–V characteristics of the MGF–ZnO contact at a given bias.[12–15] This suggests that the MGF is a promising candidate as an electrode in ZnO NW-based devices to replace commonly used metals, such as Al, Ti, Au, and Pt.

In order to understand the electrical properties of the MGF–ZnO NW contact, a physics-based model can be considered. From the Schottky contact model, the tunneling parameter E_{00} that determines the relative dominance of tunneling and thermionic emission is defined as

$$E_{00} = \frac{qh}{4\pi}\sqrt{\frac{N_D}{m^*\varepsilon_s}}, \quad (4)$$

where h is Planck's constant, m^* ($= 0.24m_0$), and ε_s ($= 8.66\varepsilon_0$) are the electron effective mass and the permittivity of the ZnO NW, respectively.[16–18] It is well known that the thermionic-field emission (TFE) process is dominant when $E_{00} \approx kT$, where k is Boltzmann's constant and T is the temperature.[6] Combining Eqs. (1) and (4), $E00$ in this study is calculated to be ~47 meV, which is similar to the thermal energy (kT) of 25 meV at $T = 300$ K. This result indicates that tunneling plays an important role in the current transport and that the TFE mechanism is the dominant process at the MGF–ZnO NW Schottky contact. For Schottky contacts, the TFE-dominated contact resistance is given by

$$R_C = \left(\frac{dI}{dV}\right)^{-1}_{V=0}$$
$$= \frac{1}{\pi r_{nw}^2}\frac{k\sqrt{E_{00}}\cosh\left(\frac{E_{00}}{kT}\right)\coth\left(\frac{E_{00}}{kT}\right)}{A^*Tq\sqrt{\pi q(\Phi_{Bn}-\xi)}}\exp\left[\frac{q\xi}{kT} + \frac{q(\Phi_{Bn}-\xi)}{E_{00}\coth\left(\frac{E_{00}}{kT}\right)}\right]. \quad (5)$$

Here, A^* ($= 32\,A\,K^{-2}\,cm^{-2}$) is Richardson's constant for *n*-type ZnO, Φ_{Bn} is the effective barrier height at zero bias, and ξ is the measured conduction band minimum (E_C) of the NW with respect to the energy of the Fermi level (E_F).[16,19] The ξ value can be estimated from the relation $\xi = (E_C - E_F) = (kT/q)\ln(N_C/N_D)$, where $N_C = 4.49 \times 10^{18}\,cm^{-3}$ is the effective density of states of the ZnO conduction band.[16,17] The zero-voltage slope of the I–V curve of a representative MGF–ZnO NW–Al device (Figure 2(a); red triangles) is fitted quantitatively using Eq. (5), with $\Phi_{Bn} = 0.413$ eV obtained from the MGF–ZnO NW Schottky contact. Note that the extracted zero-bias barrier height from the measured data is higher than the value predicted theoretically ($\Phi_{Bn} = \Phi_M - \chi_{ZnO} = 0.3 \pm 0.2$ eV).

The discrepancy between the predicted and measured Φ_{Bn} values of the MGF–ZnO NW contact can be explained as follows. The barrier heights at the ZnO-electrode interface are known to be significantly influenced by not only the energy band line-up (Schottky–Mott limit) but also other factors such as the surface defect states, Fermi level pinning, and chemical reactions at the metal–ZnO interface.[20] In particular, the interface quality at the metal–NW junction in nanoscale devices plays a major role in determining the Schottky barrier height due to the high surface-to-volume ratio of the NWs. Recent studies on ZnO and In_2O_3 NW-based Schottky barrier field-effect transistors have shown that

modifying impurities, interface traps, and fixing charges at the NW-to-metal contacts change the barrier height by 0.06 eV, leading to significant changes in the device performance metrics such as the on-current and low-field channel conductance.[21,22] In the present study, along with the energy band line-up, the interface quality determined from the trap density and fixed charges at the MGF–ZnO contact are expected to determine the effective barrier height.

The low extracted ρ_c value of the MGF–ZnO contact can be attributed to several effects. A low ρ_c can be realized by lowering the barrier height to increase the current over the barrier or enhancing the carrier tunneling through the barrier.[16] In NW-based Schottky contacts with small contact areas, the electric field near the contact interface and depletion region can be higher due to the small junction area, leading to image-force lowering of the barrier height and increased tunneling. For example, a barrier lowering of 0.06 eV has been reported in Au–ZnO NW diodes wherein the maximum electric field (E_m) near the contact is 10^4 V/cm.[23] Furthermore, as the TFE mechanism dominates the electrical transport at the MGF–ZnO NW contact barrier, the calculated Φ_{Bn} is expected to be lowered further by[19]

$$\Delta\Phi_{Bn,TFE} = \left(\frac{3E_{00}}{2}\right)^{\frac{2}{3}} (V_A)^{\frac{1}{3}} \qquad (6)$$

under an applied bias (V_A). For V_A values of 0.2, 0.4, and 0.6 V, the barrier is expected to be lowered by 0.10, 0.12, and 0.14 eV, respectively; consequently, this results in an improved electrical transparency at the contacts with increasing bias. Studies have reported that when reactive metals such as Al or Ti are in contact with ZnO, the Al and Ti atoms can react with the oxygen in ZnO to form interface defects that increase the doping density of the semiconductor, thus resulting in thin Schottky barriers that improve tunneling.[24] Although recent studies have shown that there is no such C, Zn, and O atom inter-diffusion between graphene and ZnO, the tunneling current is expected to be more significant at the MGF–ZnO contact due to the graphene to NW geometry.[25] When the Schottky junction area is smaller than the depletion width, the electric fields are enhanced near the contact resulting in increased carrier tunneling through the barrier.[26] For small Schottky contact areas, the Schottky contact formed between the MGF electrode and the *in situ* grown ZnO NWs shows near-ohmic *I–V* characteristics due to the huge impact of tunneling that leads to high currents and low resistances.

In addition to the high electrical transparency of the contact, another advantage of using the MGF as the electrode at the ZnO NW contact is the formation of nanoscale contacts. Realization of high-density devices requires high-quality contacts with a minimized lateral area. It has been reported both experimentally and analytically that large three-dimensional metal electrodes connected to NWs often result in detrimental short-channel effects due to the large fringing fields near the electrode–NW interface when NWs are integrated into gated transistors.[27] Hence, considerable effort has been spent on forming nanoscale contacts in NW transistors, primarily by using thermal annealing to diffuse the metal into the semiconducting NWs; the thermal annealing forms highly conductive nanoscale alloys near the contact region to reduce the fringing effect of the large contact-to-gate coupling, decreases the drain capacitance, and weakens the drain-induced barrier lowering.[28] In our study, since the MGF electrode thickness is expected to be comparable to or thinner than the ZnO NW diameter, we expect that a nanoscale contact between the MGF and ZnO NW can be readily formed in order to reduce fringing effects near the contact; no additional experiments to precisely control the annealing conditions to determine the diffusion length effectively, and hence the channel length, will be required.

In summary, we have investigated the junction properties of semiconducting ZnO NW and graphene contacts. Chemical vapor deposition was used to diffuse the ZnO source material onto the MGF surface by exposing only the MGF side and using SiO_2 as a blocking layer. ZnO NWs were then grown from the high-energy point. A single ZnO NW was grown directly from the MGF and could be easily used to fabricate device structures. The semiconducting ZnO NW contact with the MGF exhibited a near-ohmic conductance with specific contact resistances that are comparable to or lower than those in the commonly used metal–ZnO NW configuration. Further, our analysis has revealed that the current–voltage relationship of the MGF–ZnO NW contact can be modeled as a nano-Schottky barrier in which the electrical transport is dominated by the thermionic-field emission mechanism. We believe that MGF–ZnO NW contacts with small contact areas will be useful for next-generation devices, and moreover, MGF has been shown to be a promising candidate for future transparent displays based on ZnO NW transistors.

[1]X. Wang, L. Zhi, and K. Müllen, Nano Lett. **8**, 323 (2008).
[2]K. S. Kim, Y. Zhao, H. Jang, S. Y. Lee, J. M. Kim, K. S. Kim, J.-H. Ahn, P. Kim, J.-Y. Choi, and B. H. Hong, Nature **457**, 706 (2009).
[3]Z.-S. Wu, W. Ren, D.-W. Wang, F. Li, B. Liu, and H.-M. Cheng, ACS Nano **4**, 5835 (2010).
[4]S. Kim, H. Choi, M. Jung, S.-Y. Choi, and S. Ju, Nanotechnology **21**, 425203 (2010).
[5]H. Kim, H. Choi, S.-Y. Choi, and S. Ju, J. Phys. Chem. C **115**, 22163 (2011).
[6]S. Y. Kim, H. W. Jang, J. K. Kim, C. M. Jeon, W. I. Park, G.-C. Yi, and J.-L. Lee, J. of Electron. Mater. **31**, 868 (2002).
[7]H. Sheng, N. Emanetoglu, S. Muthukumar, S. Feng, and Y. Lu, J. Electron. Mater. **31**, 811 (2002).
[8]H. Kim, J.-H. Park, M. Suh, J. R. Ahn, and S. Ju, Appl. Phys. Lett. **100**, 063112 (2012).
[9]A. Kolmakov and M. Moskovits, Annu. Rev. Mater. Res. **34**, 151 (2004).
[10]Y.-F. Lin and W.-B. Jian, Nano Lett. **8**, 3146–3150 (2008).
[11]S. E. Mohney, Y. Wang, M. A. Cabassi, K. K. Lew, S. Dey, J. M. Redwing, and T. S. Mayer, Solid-State Electron. **49**, 227–232 (2005).
[12]M.-S. Oh, D.-K. Hwang, J.-H. Lim, Y.-S. Choi, and S.-J. Park, Appl. Phys. Lett. **91**, 042109 (2007).
[13]Y. R. Ryu, T. S. Lee, J. H. Leem, and H. W. White, Appl. Phys. Lett. **83**, 4032 (2003).
[14]B. J. Coppa, R. F. Davis, and R. J. Nemanich, Appl. Phys. Lett. **82**, 400–402 (2003).
[15]B. Angadi, H. C. Park, H. W. Choi, J. W. Choi, and W. K. Choi, J. Phys. D: Appl. Phys. **40**, 1422 (2007).
[16]S. M. Sze and K. K. Ng, *Physics of Semiconductor Devices*, 3rd ed. (Wiley, New Jersey, 2007).

[17]J. B. Baxter and C. A. Schmuttenmaer, J. Phys. Chem. B **110**, 25229 (2006).

[18]J. Yoon, W.-K. Hong, M. Jo, G. Jo, M. Choe, W. Park, J. I. Sohn, S. Nedic, H. Hwang, M. E. Welland, and T. Lee, ACS Nano **5**, 558 (2011).

[19]E. H. Rhoderick and R. H. Williams, *Metal–Semiconductor Contacts*, 2nd ed. (Clarendon, Oxford, 1988).

[20]L. J. Brillson and Y. J. Lu, J. Appl. Phys. **109**, 121301 (2011).

[21]S. Kim, S. Kim, P. Srisungsitthisunti, C. Lee, M. Xu, P. D. Ye, M. Qi, X. Xu, C. Zhou, S. Ju, and D. B. Janes, J. Phys. Chem. C **115**, 17147 (2011).

[22]S. Kim, C. Delker, P. Chen, C. Zhou, S. Ju, and D. B. Janes, Nanotechnology **21**, 145207 (2010).

[23]S. N. Das, J.-H. Choi, J. P. Kar, K.-J. Moon, T. I. Lee, and J.-M. Myoung, Appl. Phys. Lett. **96**, 092111 (2010).

[24]H.-K. Kim, K.-K. Kim, S.-J. Park, T.-Y. Seong, and I. J. Adesida, J. Appl. Phys. **94**, 4225–4227 (2003).

[25]W. M. Choi, K.-S. Shin, H. S. Lee, D. Choi, K. Kim, H.-J. Shin, S.-M. Yoon, J.-Y. Choi, and S.-W. Kim, Nano Res. **4**, 440–447 (2011).

[26]G. D. J. Smit, S. Rogge, and T. M. Klapwijk, Appl. Phys. Lett. **80**, 2568–2570 (2002).

[27]J. Hu, Y. Liu, C. Z. Ning, R. Dutton, and S.-M. Kang, Appl. Phys. Lett. **92**, 083503 (2008).

[28]Y. Hu, J. Xiang, G. Liang, H. Yan, and C. M. Lieber, Nano. Lett. **8**, 925 (2008).